Journal of Nano- and Electronic Physics
Vol. **14** No 4, 04010(6pp) (2022)

Журнал нано- та електронної фізики
Том **14** № 4, 04010(6cc) (2022)

Optical Characterization of Colloidal $AgInS_2$ Quantum Dots Synthesized from Aqueous Solutions

B.V. Lopushanska[1], Y.M. Azhniuk[1,2], I.P. Studenyak[1], V.V. Lopushansky[2], A.V. Gomonnai[1,2], D.R.T. Zahn[3]

[1] *Uzhhorod National University. 46, Pidhirna St., 88000 Uzhhorod, Ukraine*
[2] *Institute of Electron Physics, NASU, 21, Universytetska St., 88017 Uzhhorod, Ukraine*
[3] *Semiconductor Physics, Chemnitz University of Technology, D-09107, Chemnitz, Germany*

(Received 24 April 2021; revised manuscript received 09 August 2022; published online 25 August 2022)

Colloidal $AgInS_2$ quantum dots (QDs) with intense broadband photoluminescence (PL) were synthesized in aqueous solutions in the presence of glutathione at mild conditions. Size-selective fractioning of QDs was performed by repeated centrifugation of the colloidal solution with the addition of 2-propanol. Based on the optical absorption and PL data, the dependences of the band gap and the PL maximum position on the QD size are analyzed. The Raman spectra of $AgInS_2$ QDs exhibit only a slight variation with decreasing QD size explained by phonon confinement. Changes in the Raman spectra with increasing laser power density are most likely related to photoinduced oxidation of the $AgInS_2$ QD surface with the formation of S–O bonds.

Keywords: Quantum dots, Colloidal synthesis, Absorption, Photoluminescence, Raman spectroscopy.

DOI: 10.21272/jnep.14(4).04010 PACS number: 78.67.Hc

1. INTRODUCTION

Semiconductor quantum dots (QDs) of the I-III-VI_2 system (in particular, $AgInS_2$) were synthesized as an alternative to well-studied binary II-VI and IV-VI QDs to avoid toxic cadmium- and lead-containing components [1-5]. The great interest towards these materials within the recent decade is driven by their intense broadband luminescence which can be tuned across the visible spectral range by the variation of size and chemical composition and prospective applications in light-emitting diodes, biomedicine, photovoltaic solar cells, and photocatalysis [1-7]. Well-elaborated high-temperature organic-based approaches with heating-up and hot-injection synthetic routes result in hydrophobic I-III-VI_2 QDs [6, 7]. In order to obtain water-soluble QDs required, in particular, for biomedical applications, the QDs are coated with amphiphilic materials to enable phase transfer from organic to aqueous media with subsequent functionalization of the QD surface with biomolecules [8]. An alternative approach to produce ternary QDs in aqueous media in the presence of mercaptoacetic acid (MAA) [8-10] or glutathione (GSH) [11-13] provides strong binding of the organic molecules to the QD surface by a mercapto group and simultaneously prevents the QDs from aggregation in water due to the electrostatic repulsion between the carboxyl anions [5, 14].

The luminescent properties of the synthesized QDs can be improved by noticeable deviations from the stoichiometric QD composition [5, 10, 13] as well as by doping with zinc or forming a ZnS shell around the Ag-In-S QD core [4, 6, 8, 9, 11, 12]. A donor-acceptor model often applied to explain the photoluminescence (PL) in Ag-In-S QDs [1, 3, 15], similarly to binary II-VI QDs of a similar size [16], however, does not describe the PL quantum yield, temperature dependence, decay characteristics as well as PL bandwidth independence of the QD size [1, 5, 10, 13, 17, 18]. Therefore, an alternative model of self-trapped excitons was suggested where one of the photogenerated carriers is localized at a certain lattice site. This leads to lattice distortion and strong electron-phonon interaction, and the broadband PL is treated as a series of phonon replicas of the pure excitonic (no-phonon) emission band [5, 15, 18]. This broadband PL characterizes individual QDs and is only slightly affected by the QD ensemble [5, 18].

The essential role of the electron-phonon interaction for the PL mechanism in Ag-In-S QDs implies the importance of studying their phonon spectra which are most efficiently probed by Raman spectroscopy. Raman spectra of non-stoichiometric Ag-In-S QDs were reported recently [10, 19, 20], including a detailed targeted study [21]. Several studies were devoted to the phonon spectra of stoichiometric $AgInS_2$ QDs [4, 6, 9], in most cases a quite limited number of spectra were presented, and analysis was encumbered by low signal-to-noise ratios and strong PL backgrounds.

Here we report on brightly luminescent $AgInS_2$ colloidal QDs synthesized in aqueous solutions with GSH and their size-selective precipitation from as-prepared polydisperse solutions with the help of a poor solvent (2-propanol). Size selected QDs are characterized by optical absorption, PL, and Raman spectroscopy.

2. EXPERIMENTAL

Synthesis of colloidal $AgInS_2$ QDs was carried out in an exchange reaction between Na_2S and a mixture of Ag(I) and In(III) complexes with GSH in aqueous solutions (with the addition of NH_4OH) at 96-98 °C following a method similar to that described earlier [10, 13]. 5 ml of deionized water were mixed with 4.8 ml of 0.5 M aqueous GSH solution and 0.4 ml of 1 M aqueous $InCl_3$ solution with 0.025 ml of 0.2 M HNO_3. Then 2 ml of 0.2 M NH_4OH solution was added, after which 4.0 ml of aqueous 0.1 M $AgNO_3$ solution and 0.8 ml of 1.0 M aqueous Na_2S solution and 0.5 ml of 2.0 M aqueous

solution of citric acid were quickly added. The resulting solution acquired an intense red color. The whole procedure was performed at constant magnetic stirring. Afterwards the reaction mixture was heated in a water bath at 95-98 °C for 40 min.

The obtained crude solution of $AgInS_2$ QDs was subjected to size fractioning by repeated centrifugation for 4 min at 4000 rpm with the addition of a new portion of poor solvent (2-propanol), similarly to the procedure described by Raevskaya et al. [10]. At each subsequent stage of centrifugation, the average size of the precipitated fraction was smaller than of the previous one. After the separation each fraction was again dissolved in distilled water.

The size-selected colloidal solutions were characterized by optical absorption, PL, and Raman spectroscopy. Optical absorption spectra were recorded using a Cary 50 spectrophotometer (Varian) with a full spectrum Xe pulse lamp source and dual Si diode detectors. A Black Comet CXR-SR spectrometer (StellarNet) was used for optical absorption and PL measurements with the PL excitation provided by a $\lambda_{exc} = 390$ nm diode.

For micro-Raman studies, aqueous solutions of size-fractioned colloidal $AgInS_2$ QDs were drop-casted on silicon substrates and subsequently dried at room temperature and ambient pressure. The measurements were performed using a Horiba LabRAM HR800 spectrometer equipped with a cooled CCD camera. The excitation was provided by a solid-state laser with $\lambda_{exc} = 488$ nm. The instrumental resolution was better than 2.5 cm^{-1}. All measurements were carried out at room temperature.

3. RESULTS AND DISCUSSION

Fig. 1a shows the optical absorption spectra of size fractioned colloidal $AgInS_2$ QD solutions. Similar to earlier studies of Ag-In-S QDs [10, 13, 19], a noticeable blue shift of the absorption edge is observed with increasing fraction number as evidence for the NC size decrease. While for extensively studied II-VI QDs, for which (if the average QD size is smaller than the exciton Bohr radius) one can observe distinct size-dependent maxima in the optical absorption spectra and determine, from their spectral positions, the average QD size using the effective mass approximation [22], here we did not observe any confinement-related maxima. This fact is well known for Ag-In-S QDs and can be explained by smearing the maxima due to the strong Urbach tail absorption by defect states [10, 13, 19].

The optical absorption spectra replotted in the $(\alpha h\nu)^2$ vs $h\nu$ coordinates (where α is the absorption coefficient), appropriate for direct-band gap semiconductors, enable the band gap value E_g to be determined for each fraction by extrapolating the extended linear section to intercept the energy axis. The corresponding E_g values are shown in Fig. 2. In recent studies of size-selected Ag-In-S QDs, good correlation of the QD size evaluated from thus determined E_g and the value estimated from transmission electron microscopy (TEM) [10] and atomic force microscopy (AFM) [20] was reported.

Except for the first two fractions with the biggest QDs, $AgInS_2$ QDs exhibit an intense broad PL maximum (Fig. 1b). Similar broadband PL was observed earlier for $AgInS_2$ QDs prepared by a variety of chemical routes [1, 2, 4, 6, 9, 12]. The luminescent properties of $AgInS_2$ as well as related core/shell $AgInS_2$/ZnS QDs are often explained within a donor-acceptor PL model [1, 3, 6, 11, 15], according to which the photogenerated charge carriers are quickly trapped by lattice defects as well as surface states that can introduce local states within the band gap and afterwards recombine radiatively or nonradiatively with free/trapped carriers of opposite charge or detrapped by thermal activation or recombine via a tunneling mechanism [5]. The radiative recombination of these electron-hole pairs results in the emission of photons with an energy distribution broadened by inhomogeneities in QD size and chemical composition, as well as the distribution in depth/energy position of trap states and distances between trapped electrons and holes within a single particle [16].

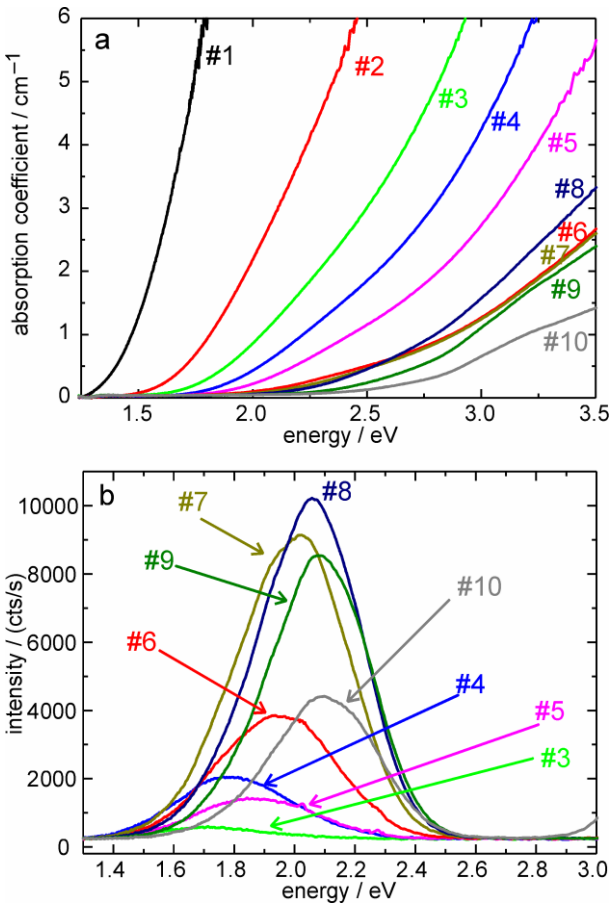

Fig. 1 – Optical absorption (a) and PL (b) spectra of a series of size-fractioned GSH-capped $AgInS_2$ QD solutions

It can be seen from Fig. 1b that the spectral width of the PL band practically does not depend on the fraction number (i.e., the average QD size). Similar size independence of the PL bandwidth was observed earlier [1]. It was also shown that the $AgInS_2$ QD PL width does not vary with temperature and excitation intensity [1], even though the distribution of the emissive centers formed upon light absorption was expected to be changed by these factors. An alternative model of self-trapped excitons is more appropriate to explain the luminescent properties of Ag-In-S QDs [5]. According to this model, one of the photogenerated carriers is localized at a certain lattice site resulting in lattice distor-

tion and strong electron-phonon interaction [15]. The broadband PL is treated as a series of phonon replicas of the pure excitonic (zero-phonon) emission line [18]. Such broadband luminescence is considered to originate from the whole QD lattice, not from individual defects and is an inherent property of single QDs, only slightly affected by the QD ensemble [5, 18].

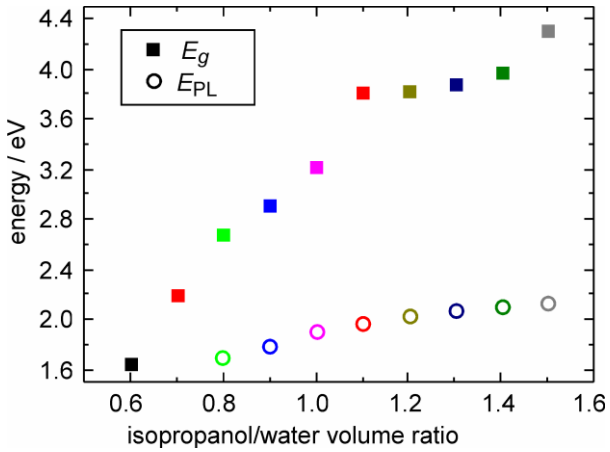

Fig. 2 – Dependences of the bandgap E_g and PL maximum position E_{PL} on the 2-propanol/water volumetric ratio for a series of size-fractioned GSH-capped $AgInS_2$ QD solutions

With increasing fraction number (decreasing QD size) the PL maximum shifts towards higher energies (Fig. 1b). In our recent study [19], we found it appropriate to attribute the reduction in QD size to the volumetric ratio of 2-propanol and water for each fraction rather than to the non-informative fraction number. This enables one not only to analyze the data within one size-selected QD series, but also to compare them for different batches of similar composition. The corresponding dependences of the band gap and PL maximum position shown in Fig. 2 visualize the increasing Stokes shift with decreasing QD size. The PL maximum shift with the 2-propanol to water volumetric ratio is found to be much smaller than that of the absorption edge (Fig. 2) which means a large Stokes shift increasing with decreasing QD size. This fact is consistent with recent observations for size-fractioned non-stoichiometric Ag-In-S QDs [5, 19].

Raman measurements of $AgInS_2$ QDs [4, 6, 9] as well as non-stoichiometric Ag-In-S QDs [10, 19-21] were reported in earlier studies. In most publications, a very limited number of spectra were presented, and their analysis was hampered by low signal-to-noise ratios and strong luminescence background. A more detailed discussion of the phonon spectra was performed in a recent targeted Raman and infrared study of Ag-In-S QDs in comparison with their Cu-In-S and Hg-In-S counterparts [21] as well as a recent paper devoted to Cu → Ag substitution in quaternary Cu(Ag)-In-S QDs [20]. In these two publications, spectra with much better signal-to-noise ratio were reported, in particular, due to adding methylviologen to the colloidal solution which served as an efficient PL quencher [20, 21]. However, to our knowledge, no analysis of the effect of the $AgInS_2$ QD size on their Raman spectra has been presented so far. It should be noted that in our case, although the energies of the broadband PL peak maxima (Fig. 1b) were noticeably below the Raman excitation energy (2.54 eV), the PL background in the Raman measurements was quite intense and the analysis required a thorough baseline subtraction procedure.

The Raman spectra of the size-fractioned series of $AgInS_2$ QDs, shown in Fig. 3, reveal quite broad features in the range from 100 to 450 cm^{-1} (first-order Raman scattering) and a broad continuum at 500-700 cm^{-1} (second-order). Contrary to II-VI QDs, where Raman features are much narrower [23], for tetragonal $AgInS_2$ and $CuInS_2$ QDs [4, 6, 9] as well as for related non-stoichiometric Ag-In-S and Cu-In-S QDs [10, 19-21] such broad features are quite typical. Such character of the Raman spectra is explained by a more complicated set of phonon modes which can noticeably overlap [21] as well as by confinement-related Raman band broadening and surface phonon scattering, the contribution of which increases for small QDs [23].

The lowest-frequency Raman peak at 126-133 cm^{-1} was observed earlier, besides our recent studies of non-stoichiometric Ag-In-S QDs [19, 20], only by Borkovska et al. [9], while other authors did not report Raman measurements in this frequency range. This peak is attributed to In–S bond vibrations. A peak at a somewhat higher frequency of 168-175 cm^{-1} was not reported previously for $AgInS_2$ QDs but was clearly observed for non-stoichiometric Ag-In-S QDs and assigned to Ag–S vibrations [19, 20].

The frequency range 200-400 cm^{-1} contains broad Raman features which were observed with a slightly different intensity distribution in earlier studies of $AgInS_2$ [4, 6, 9] as well as non-stoichiometric Ag-In-S [10, 19-21] QDs. They are composed of a series of overlapping modes which were studied in detail by Dzhagan et al. [21] including symmetry assignment for some peaks and temperature behavior. According to our analysis [19, 20], both Ag–S and In–S bond vibrations contribute to the Raman scattering intensity in this frequency interval. In view of the evident large width of features and a sufficient set of oscillators contributing to scattering in this spectral range [21, 24], multi-peak simulation of the observed spectra can be performed quite arbitrarily and does not seem reliable. Hence, we concentrated on the most obvious changes observed in the spectra for different size fractions.

It can be clearly seen that the two first fractions with the largest QDs reveal spectra somewhat different from the others, while the spectra of finer fractions look almost identical. The scattering intensity in the range 200-400 cm^{-1} changes its shape without clearly revealed features for fractions #1 and #2, while for fractions #3 to #10 it becomes more clearly shaped with two broad maxima near 270-280 cm^{-1} and 335 cm^{-1} as well as a rather featureless high-frequency continuum, extending even beyond 450 cm^{-1} which increases in intensity with fraction number (decreasing QD size). One can assume that scattering in this high-frequency region is related to nonzero-wavevector $q \neq 0$ phonons, the participation of which in the first-order Raman scattering becomes possible in QDs because of the selection rule relaxation due to phonon confinement. This correlates well with calculated data that predict the dispersion of $AgInS_2$ phonons in this range with frequency increasing at $q \neq 0$ [24].

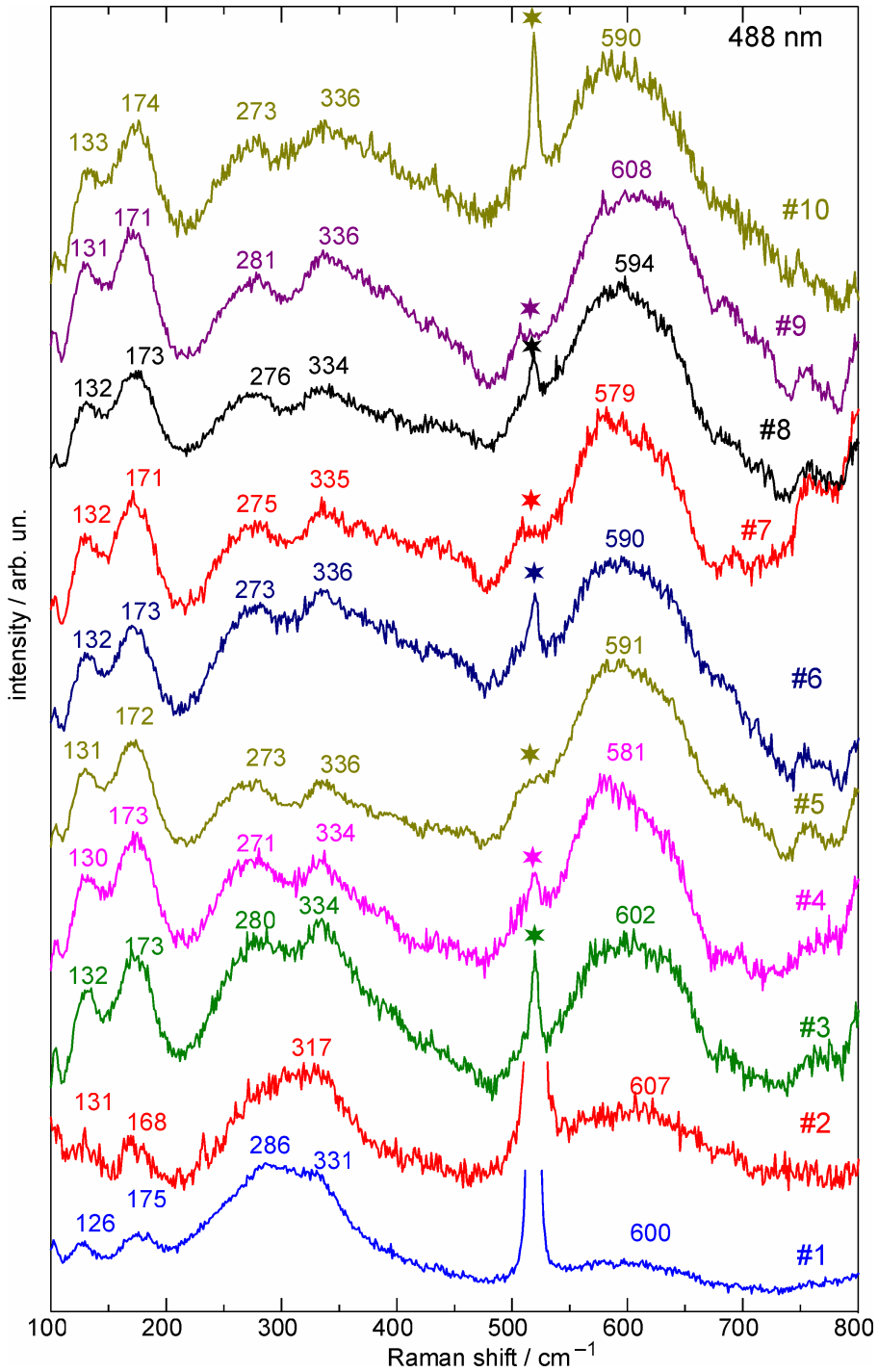

Fig. 3 – Raman spectra of size-fractioned $AgInS_2$ QDs. The fraction numbers are indicated at each curve. The peak at 520 cm^{-1} corresponds to the silicon substrate

Besides, it can be seen from Fig. 3 that for the first two fractions, the relative intensities of the lower-frequency bands near 130 cm^{-1} (In–S bond vibrations) and 170 cm^{-1} (Ag–S bond vibrations) are considerably lower with respect to higher-frequency maxima than for higher fractions with smaller QD size. One may assume that phonon confinement favors the intensity increase of these two peaks for smaller QDs, although we cannot find a reasonable argument why the intensities of the lower-frequency bands should increase much more noticeably than for smaller QDs. Besides, it should be kept in mind that, contrary to fractions #1 and #2, for which no PL was observed, the spectra of finer QD fractions were subjected to a PL background subtraction procedure, which could also affect the intensity distribution.

A broad maximum near 600 cm^{-1} is related to two-phonon processes. Its intensity noticeably increases with the QD size decrease. This is most likely related to an increasing exciton-phonon interaction for smaller QDs which correlates with the Stokes shift increase (see Fig. 2).

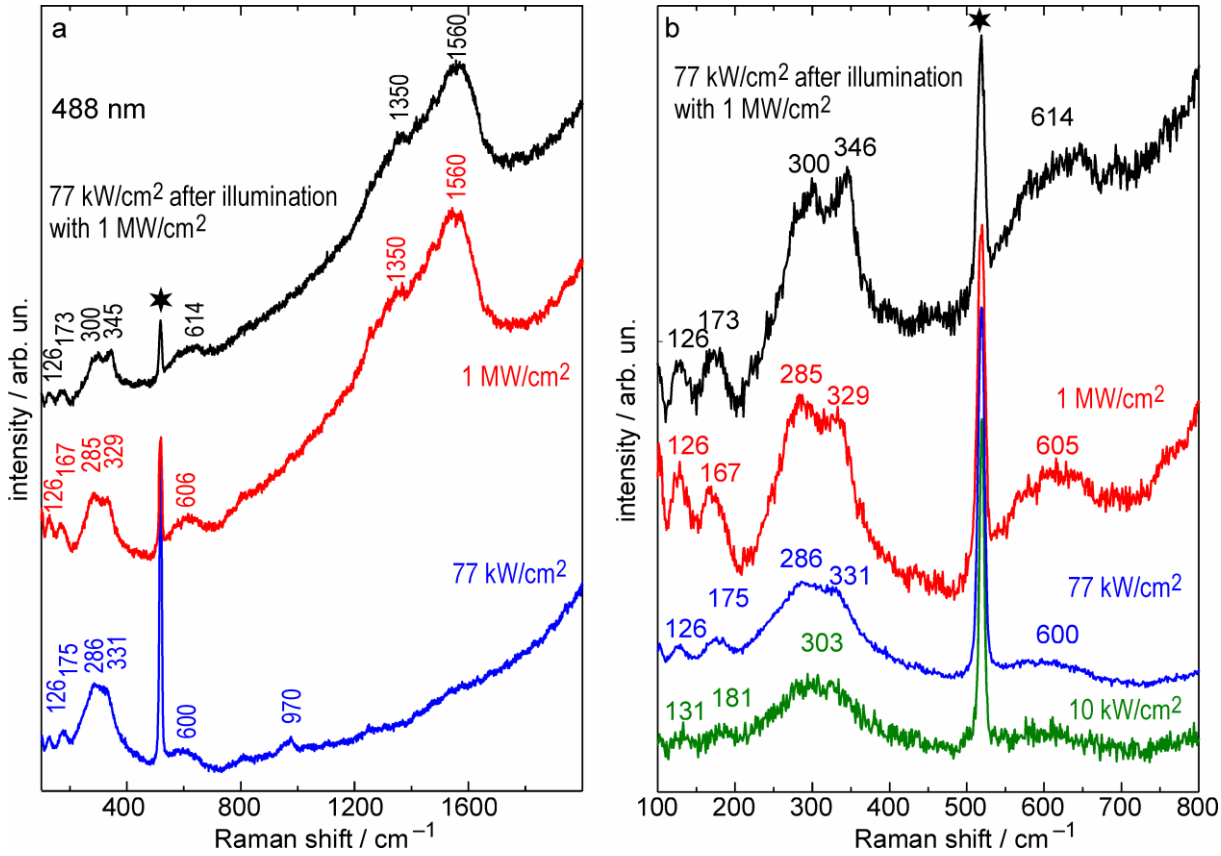

Fig. 4 – Raman spectra of $AgInS_2$ QDs fraction #1 under excitation with different laser power densities. Panel (b) is a zoomed-in lower-frequency part of panel (a). The peak at 520 cm^{-1} corresponds to the silicon substrate

It can be seen from a more detailed view in Fig. 4b that after illumination by $P_{exc} = 1$ MW/cm² not only the high-frequency bands related to the sulfur oxidation on the QD surface appear, but also the most intense relatively broad maxima at 286 and 331 cm^{-1} in the $AgInS_2$ QD spectrum shift toward higher frequencies by about 15 cm^{-1}. This shift qualitatively correlates with the corresponding shift of the two-phonon maximum from 600 to 616 cm^{-1}. Due to a complex nature of the Raman features in the range 200-400 cm^{-1} it is difficult to determine unambiguously which $AgInS_2$ vibrations are directly affected by the photochemical transformation.

4. CONCLUSIONS

$AgInS_2$ QDs capped with glutathione were prepared by colloidal synthesis in aqueous solutions under mild conditions. Size-selected fractions of the colloidal solutions prepared by repeated centrifuging with stepwise addition of 2-propanol are characterized by the Urbach absorption edge and intense broadband PL. The size dependences of the optical band gap and the PL maximum position reveal a monotonous increase in the Stokes shift with decreasing QD size.

The Raman spectra of $AgInS_2$ QDs exhibit slight variation with decreasing QD size explained by phonon confinement. New intense Raman bands near 1350 and 1560 cm^{-1} observed at increased laser power density ($P_{exc} = 1$ MW/cm²) and retained in the spectra after the power density is reduced back, are most likely related to the photoinduced oxidation of $AgInS_2$ QD surface with the formation of S–O bonds. The high-frequency shift of the Raman features of $AgInS_2$ QDs in the range 200-400 cm^{-1} after illumination with $P_{exc} = 1$ MW/cm² requires a detailed study.

ACKNOWLEDGEMENTS

The authors are much obliged to O. Raievska and O. Stroyuk for helpful advice and discussion, as well as to Ya.I. Lopushanska, Ya.I. Studenyak and A.I. Pogodin for assistance at the synthesis stage. Y.M. Azhniuk is grateful to Chemnitz University of Technology (Visiting Scholar Program) for supporting his research fellowship at the university.

REFERENCES

1. Y. Hamanaka, T. Ogawa, M. Tsuzuki, *J. Phys. Chem. C* **115**, 1786 (2011).
2. K.P. Kadlag, P. Patil, M. Jagadeeswara Rao, S. Datta, A. Nag, *CrystEngComm* **16**, 3605 (2014).
3. Y. Hamanaka, K. Ozawa, T. Kuzuya, *J. Phys. Chem. C* **118**, 14562 (2014).
4. B. Cichy, R. Rich, A. Olejniczak, Z. Gryczynski, W. Strek, *Nanoscale* **8**, 4151 (2016).

5. *Core/Shell Quantum Dots. Lecture Notes in Nanoscale Science and Technology* (Ed. X. Tong, Z.M. Wang) (Springer: 2020).
6. S.P. Hong, H.K. Park, J.H. Oh, H. Yang, Y.R. Do, *J. Mater. Chem.* **22**, 18939 (2012).
7. T. Torimoto, M. Tada, M. Dai, T. Kameyama, S. Suzuki, S. Kuwabata, *J. Phys. Chem. C* **116**, 21895 (2012).
8. M.D. Regulacio, K.Y. Win, S.L. Lo, S.Y. Zhang, X. Zhang, S. Wang, M.Y. Han, Y. Zheng, *Nanoscale* **5**. 2322 (2013).
9. L. Borkovska, A. Romanyuk, V. Strelchuk, Y. Polishchuk, V. Kladko, O. Stroyuk, A. Raevskaya, T. Kryshtab, *Mater. Sci. Semicond. Proc.* **37**, 135 (2015).
10. A. Raevskaya, V. Lesnyak, D. Haubold, V. Dzhagan, O. Stroyuk, N. Gaponik, D.R.T. Zahn, A. Eychmüller, *J. Phys. Chem. C* **121**, 9032 (2017).
11. Z. Luo, H. Zhang, J. Huang, X. Zhong, *J. Colloid Interface Sci.* **377**, 27 (2012).
12. W.W. Xiong, G.H. Yang, X.C. Wu, J.J. Zhu, *J. Mater. Chem. B* **1**, 4160 (2013).
13. O. Stroyuk, A. Raevskaya, F. Spranger, O. Selyshchev, V. Dzhagan, S. Schulze, D.R.T. Zahn, A. Eychmüller, *J. Phys. Chem. C* **122**, 13648 (2018).
14. L. Jing, S.V. Kershaw, Y. Li, X. Huang, Y. Li, A.L. Rogach, M. Gao, *Chem. Rev.* **116**, 10623 (2016).
15. D. Aldakov, A. Lefrançois, P. Reiss, *J. Mater. Chem. C* **1**, 3756 (2013).
16. V. Lesnyak, N. Gaponik, A. Eychmüller, *Chem. Soc. Rev.* **42**, 2905 (2013).
17. O. Stroyuk, V. Dzhagan, A. Raevskaya, F. Spranger, N. Gaponik, D.R.T. Zahn, *J. Lumin.* **215**, 116630 (2019).
18. O. Stroyuk, F. Weigert, A. Raevskaya, F. Spranger, C. Würth, U. Resch-Genger, N. Gaponik, D.R.T. Zahn, *J. Phys. Chem. C* **123**, 2632 (2019).
19. B.V. Lopushanska, Yu.M. Azhniuk, V.V. Lopushansky, Sh.B. Molnar, I.P. Studenyak, O.V. Selyshchev, D.R.T. Zahn, *Appl. Nanosci.* **10**, 4909 (2020).
20. O. Raievska, O. Stroyuk, Y. Azhniuk, D. Solonenko, A. Barabash, C.J. Brabec, D.R.T. Zahn, *J. Phys. Chem. C* **124**, 19375 (2020).
21. V. Dzhagan, O. Selyshchev, O. Raievska, O. Stroyuk, L. Hertling, N. Mazur, M.Ya. Valakh, D.R.T. Zahn, *J. Phys. Chem. C* **124**, 15511 (2020).
22. A.L. Rogach, A. Kornowski, M. Gao, A. Eychmüller, H. Weller, *J. Phys. Chem. B* **103**, 3065 (1999).
23. V.M. Dzhagan, Yu.M. Azhniuk, A.G. Milekhin, D.R.T. Zahn, *J. Phys. D: Appl. Phys.* **51**, 503001 (2018).
24. G. Petretto, S. Dwaraknath, H.P.C. Miranda, D. Winston, M. Giantomassi, M.J. van Setten, X. Gonze, K.A. Persson, G. Hautier, G.-M. Rignanese, *Sci. Data* **5**, 180065 (2018).
25. R.J. Gillespie, E.A. Robinson, *Canad. J. Chem.* **40**, 658 (1962).

Оптичні характеристики колоїдних квантових точок $AgInS_2$, синтезованих з водних розчинів

Б.В. Лопушанська[1], Ю.М. Ажнюк[1,2], І.П. Студеняк[1], В.В. Лопушанський[2], О.В. Гомоннай[1,2], Д.Р.Т. Цан[3]

[1] *Ужгородський національний університет, вул. Підгірна, 46, 88000, Ужгород, Україна*
[2] *Інститут електронної фізики НАН України, вул. Університетська, 21, 88017, Ужгород, Україна*
[3] *Фізика напівпровідників, Кемніцький технічний університет, D-09107, Кемніц, Німеччина*

Колоїдні квантові точки (КТ) $AgInS_2$ з інтенсивною широкосмуговою фотолюмінесценцією (ФЛ) синтезовано у водних розчинах у присутності глутатіону при помірних умовах. Розділення КТ на фракції за розміром проведено багаторазовим центрифугуванням колоїдного розчину з додаванням 2-пропанолу. На основі даних оптичного поглинання та ФЛ проводиться аналіз залежності ширини забороненої зони та максимального положення ФЛ до розміру КТ. Раманівські спектри КТ $AgInS_2$ демонструють незначні зміни зі зменшенням розміру КТ, що пояснюється просторовим обмеженням фононів. Зміни у раманівських спектрах при збільшенні густини потужності лазера найімовірніше пов'язані з фотоіндукованим окисленням поверхні КТ $AgInS_2$ з утворенням зв'язків S–O.

Ключові слова: Квантові точки, Колоїдний синтез, Поглинання, Фотолюмінесценція, Раманівська спектроскопія.